Published in final edited form as:
Circ Res. 2009 June 5; 104(11): 1260–1266. doi:10.1161/CIRCRESAHA.108.191718.

Genetic evidence for a non-canonical function of seryl-tRNA Synthetase in vascular development

Wiebke Herzog[1,2], **Katja Müller**[2], **Jan Huisken**[1], and **Didier Y. R. Stainier**[1,*]

[1] Dept. of Biochemistry and Biophysics, and the Cardiovascular Research Institute, Programs in Developmental Biology, Genetics, and Human Genetics, University of California San Francisco

[2] Westphalian Wilhelms University and Max-Planck Institute for Molecular Biomedicine, Muenster, Germany

Abstract

In a recent genetic screen, we identified mutations in genes important for vascular development and maintenance in zebrafish [1]. Mutations at the *adrasteia* (*adr*) locus cause a pronounced dilatation of the aortic arch vessels as well as aberrant patterning of the hindbrain capillaries and, to a lesser extent, intersomitic vessels. This dilatation of the aortic arch vessels does not appear to be caused by increased cell proliferation, but is dependent on Vegf signaling. By positional cloning, we isolated *seryl-tRNA synthetase* (*sars*) as the gene affected by the *adr* mutations. siRNA knockdown experiments in HUVEC cultures indicate that SARS also regulates endothelial sprouting. These analyses of zebrafish and human endothelial cells reveal a new non-canonical function of Sars in endothelial development.

Keywords

Aminoacyl-tRNA synthetases; Seryl-tRNA Synthetase; Sars; SerRS; zebrafish; angiogenesis; vascular dilatation

Introduction

The formation and maintenance of the cardiovascular system is essential for supplying nutrients and oxygen throughout the organism. To ensure survival, the vasculature needs to be able to respond quickly to hypoxic situations, e.g. during wound repair. On the other hand, an imbalance in vascular growth contributes to a large number of disorders including cancer, arthritis, blindness, ischemia and osteoporosis [2, 3]. Therefore, the development of the vasculature is highly regulated and utilizes well conserved cellular and molecular mechanisms (reviewed by [4, 5, 6]). A challenge in studying vascular development lies in the crosstalk between the vasculature and its surrounding tissues as well as in the dependence of one for the survival of the other. Whereas mammals are dependent on the vascularization of the placenta for embryonic development, zebrafish embryos have the unique advantage that they can survive without a functional vasculature, or heart beat, for up to 7 days post fertilization, that is well into free swimming larval stages [7, 8, 9]. Additionally, the optical clarity of zebrafish embryos allowing for *in vivo* analysis of fluorescent transgene expression [10] and their amenability to genetic screens [11, 12, 13] have rendered them ideal to study vascular development and identify and analyze new genes regulating that process.

* To whom correspondence should be addressed. E-mail: didier.stainier@ucsf.edu.

Disclosures: None

In this report, we analyze the effect of mutations in the zebrafish gene *adrasteia* (*adr*), and show that *adr* corresponds to the *seryl-tRNA synthetase* gene. Aminoacyl-tRNA synthetases catalyze the ligation of specific amino acids to their cognate tRNAs and thereby assemble the building blocks for RNA-translation and protein synthesis. Whereas this essential function is based on the catalytic activity of these enzymes, there is increasing evidence that these proteins are versatile and have acquired functions in processes not directly related to protein synthesis. These so called non-canonical functions range from interactions of tRNA-synthetases with themselves and other proteins in a multisynthetase complex (reviewed by [14]) to specific functions in silencing of gene translation [15] or as angiogenic or angiostatic cytokines [16, 17]. Other acquired functions of mammalian tRNA-synthetases include anti-apoptosis and translational control (reviewed by [18]).

Although their catalytic enzymatic core is highly conserved from bacteria to mammals, there is evidence that in some Aminoacyl-tRNA synthetases, new functions were acquired by appending extra domains to the core-domain [19, 20, 21]. For example, human Tyrosyl-tRNA synthetase has gained an extra C-terminal domain of ca 170 amino acids [22] that has cytokine-like effects on leukocytes and monocytes [23]. In contrast, human Tryptophanyl-tRNA synthetase acquired 60 amino acids at its N-terminus, the presence or absence of which is regulated by alternative splicing. Both of the isoforms possess aminoacylation activity, but only the shorter form also exhibits angiostatic activity – blocked by the N-terminal appendage in the longer form [16, 24]. Although Seryl-tRNA synthetase (Sars) has not been described to exhibit non-canonical activities, the vertebrate enzyme also contains a C-terminal appendage of ca 40 amino acids which appears to be a vertebrate invention (data not shown).

Here we show for the first time that Sars has indeed acquired a non-canonical function in vertebrates, one that plays a key role in vascular development.

Material and Methods

Zebrafish husbandry and positional cloning

Zebrafish (*Danio rerio*) embryos were obtained from the mixed wild-type strain in the laboratory and raised at 28°C as previously described [25].

Genomic mapping and positional cloning was performed using SSLP markers as previously described [26]. Sequences of published SSLP markers can be found at http://zebrafish.mgh.harvard.edu/.

Pharmacological manipulations and vessel diameter analysis

Embryos were treated with either 1μM SU5416 (CalBiochem) or with the indicated amounts of Cycloheximide (Sigma) or a Seryl analogue (5′-O-[N-(L-seryl)sulfamoyl]adenosine (IDT) from 60 to 72 or 74hpf. As a control, embryos from the same batch were treated with DMSO at the same concentration (0.01% -0.05%).

Embryos were imaged with selective plane illumination microscopy (SPIM) [27] or Zeiss Lumar stereo microscopy. The vessel diameter was determined with ImageJ.

The mean values are depicted, error bars denote standard deviation. Statistical significance was determined using unpaired (two sample unequal variance) t-test.

BrdU incorporation and staining

Embryos were injected with a BrdU solution (10mM BrdU, 0.2M KCl, 1% phenol red) into the pericardial sac at 58hpf, fixed in 4% PFA at 74hpf, treated with 2mM HCl for 1h, embedded

in 4% agarose and sectioned using a Leica vibratome. Sections were stained for incorporated BrdU with anti-BrdU antibody (Roche), using anti-mouse Alexa546 (Invitrogen) as secondary label. Processed samples were mounted in Vectashield (Vector Laboratories) and the images acquired using a Leica confocal microscope.

Evan's Blue Injection

Larvae were injected with a 1% Evans Blue (Sigma) solution into the circulation prior to the heart inflow (fusion of the common cardinal veins) at 74hpf, fixed in 4% PFA, embedded in 4% agarose and sectioned using a Leica vibratome. Sections were mounted in Fluoromount-G (Southern Biotech) and the images acquired using a Leica confocal microscope.

siRNA-Transfection of HUVEC

Human umbilical vein endothelial cells (HUVEC, Invitrogen) were grown in Medium 200 with Low Serum Growth Supplements (Invitrogen) according to manufacturers' instructions. They were transfected, using Oligofectamine (Invitrogen) only (mock transfection) or either 70nM or 150nM of On-Target plus SMARTpool siRNA (Thermo Scientific, #L-013477-01) against seryl-tRNA-synthetase (Acc.No. NM_006513) in OptiMEM medium (GIBCO). 16h after transfection, cells were subjected to an In Vitro Angiogenesis Assay: Tube Formation (Trevigen) according to manufacturers' instructions. Briefly, endothelial cells were evenly seeded onto a basement membrane extract and stimulated with 10ng/ml VEGF in Medium 200 with Low Serum Growth Supplements (Invitrogen). After 6h they were labeled with 2mM Calcein and visualized using a Leica Stereomicroscope using Volocity. Each experiment was carried out in triplicates. After image acquisition, the number of branchpoints was counted in equal size areas and statistical significance determined using unpaired (two sample unequal variance) t-test. The P value was considered statistically significant when ($P < 0.05$).

Results

The *adrasteia (adr)* mutations were identified in a recent genetic screen for vascular regulators [1]. *adr* mutants appear morphologically unaffected for the first 3 days of development (Fig. 1). By observing *Tg*(*flk1:*EGFP)^{s843} expression, we noticed a pronounced dilatation of the aortic arch vasculature (Fig. 1F) on day 3 (72 hours post fertilization (hpf)) and subsequent aberrant branching of the hindbrain capillary network, and to a lesser extent, the intersomitic vessels (Fig. 1J). Although initially unaffected, circulation gradually diminishes until at day 5 of development it is confined to a minimal circulatory loop (data not shown). It is important to note that at 60hpf *adr* mutants are still indistinguishable from their wild-type (wt) siblings (data not shown), so that the manifestation of the dilatation phenotype happens within 12 hours. We quantified the extent of dilatation by measuring the vessel diameter in wild-type and *adr* mutant embryos. Fig. 1H shows that in 80hpf *adr* mutants the diameter of the aortic arch vessels was increased by up to 2 fold.

To investigate the increase in vessel diameter, we analyzed cell division as well as the physical environment of the aortic arch vasculature. We labeled dividing cells by injecting BrdU into the circulation of 58hpf old embryos, allowed for incorporation until 74hpf at which time we fixed the animals. We then cut transverse sections containing the second or third visible aortic arch vessels (AA3 and AA4) and examined them for incorporated BrdU. We observed very few (0-1) cell divisions in the endothelial cells of the second or third aortic arch vessels of wild-type embryos during that time, although the surrounding tissue was very actively dividing (Fig. 2A). Likewise, no cell division was observed in the aortic arch vessels of *adr* mutants (Fig. 2B), indicating that the increase in vessel diameter is not caused by an increase in cell number. Additionally, we observed no obvious difference in the extracellular matrix as assessed by Fibronectin and Laminin expression (data not shown). Therefore it is likely that

adr mutants represent a model for vascular dilatation rather than vascular enlargement, the latter resulting from an increase in endothelial cell number.

In order to further analyze the physical effects of the mutation, we crossed *adr* heterozygous carriers to a transgenic line expressing dsRed under the *gata1* promoter [28] so that we could examine the distribution of red blood cells in detail. No *Tg(gata1:*dsRed*)*^{sd2}-positive cells were found outside the vasculature in *adr* mutants (data not shown). We further analyzed the permeability of the vessels by injecting Evans Blue[29] into the circulation at 74hpf. After 30 minutes, we fixed the larvae, cut sagittal sections and examined them for leakage of Evans Blue in the tissue surrounding the vessel in single plane confocal sections (Fig. S1). We did not observe any obvious defect in vascular integrity in *adr* mutant larvae.

To begin to understand the process leading to this vascular dilatation, we treated embryos from 60 to 76hpf with the Vegf-Receptor inhibitor SU5416. Inhibition of Vegf signaling in *adr* mutants abolished dilatation of the aortic arch vessels, although the inhibitor did not appear to have any effect on the wild-type arch vasculature (Fig. 2C, D). Therefore, functional Vegf signaling seems to be required for the process of vascular dilatation downstream of the *adr* mutation.

To isolate the gene affected by the *adr* mutations, we used simple sequence length polymorphisms (SSLP) for mapping and subsequent positional cloning. We located *adr* on Linkage group 23 (LG23), between z20725 and Z5141, 34cM – 36.6 from the top of the linkage group (MGH map). Consecutive mapping with individually selected SSLP markers placed *adr* on the FPC contig 2305 within close proximity of the *seryl-tRNA-synthetase* (*sars*) gene. By sequencing cDNAs from wild-type and mutant *adr* embryos, we found significant mutations in the *sars* gene in each of the two *adr* alleles identified. The *sars*^{s277} allele shows a T_{1194} to G transition, which replaces the highly conserved Phenylalanine (F^{383}) with a Valine. The phenylalanine at this position is highly conserved from bacteria to human. The *sars*^{s228} allele shows a G to T transition, resulting in a premature stop codon after amino acid 420 (Fig. 3A). Additionally, another zebrafish mutation, *hi*^{3817}, identified in an insertional mutagenesis screen was found to affect the *sars* gene and described with the same breakdown of circulation at 120hpf [30]. The tight genetic linkage and existence of three different *sars* mutant alleles, all displaying the same vascular phenotype indicate that mutations in *sars* are causing the phenotype.

A well known function of Seryl-tRNA synthetase is to catalyze the ligation of serine to its cognate tRNA's, resulting in seryl-tRNA complexes necessary for translation of RNA into protein. To analyze whether the vascular phenotype observed in *adr* mutants was caused by defective protein synthesis, we chemically inhibited protein synthesis between 60 and 72hpf by addition of cycloheximide [31]. Treatment with cycloheximide led to very thin, stretched aortic arch vessels and a reduction in hindbrain capillary formation (Fig. 3C, D). We also examined the effects of a reduction of protein synthesis by using either reduced concentrations of cycloheximide or a Seryl analogue which inhibits seryl-tRNA synthetase activity [32]. We did not observe any dilatation of the aortic arch vessels or aberrant capillary patterning with either treatment (Fig. S2). Thus, reduction or lack of protein synthesis did not appear to cause vascular dilatation or aberrant capillary formation similar to the phenotypes observed in *adr* mutants. Additionally, zebrafish mutants in *methionine-* (*mars*), *lysine-* (*kars*), *glutamine-*(*qars*) and *valine-* (*vars*) *tRNA-synthetase* genes have been described [30], none of which exhibits the breakdown in circulation observed in 5 day old *sars* mutants.

To begin to analyze whether the effect of the *adr* mutations on the vasculature is endothelial cell specific, we reduced *SARS* expression in human umbilical vein endothelial cells (HUVEC) by transfection with siRNA against human *SARS*. At a concentration of 75 and 150nM siRNA

per 1×10^4 cells, we observed after 48 hours significant cell death in *SARS*-siRNA transfected but not in mock transfected HUVEC cultures. This effect was concentration dependent and could be reduced by either decreasing the amount of siRNA or by increasing the number of cells (not shown). We assume that the increased cell death is related to the general function of SARS in protein synthesis and would be observed in other cell types as well. To analyze whether *SARS*-siRNA had a specific effect on endothelial cells, we subjected HUVEC's 16 hours after transfection to a network formation assay. For this assay, endothelial cells were evenly seeded onto a gel-like extracellular matrix substitute (basement membrane extract) and after VEGF stimulation underwent a rapid reorganization, during which they migrated on the matrix, formed cell-cell contacts and formed a network within about 6 hours. Other assays[33] based on different matrices and less stimulating factors can result in complete tube formation but take several days. We elected to use the rapid network formation assay in order to minimize the effects on cell viability from knocking down *SARS*. We found a strong change in network formation and branching behavior of *SARS*-siRNA transfected HUVEC's. Reduction of SARS expression resulted in an increase in the number of tube-like structures formed (Fig. 4F) and in a much less organized pattern of these network connections (Fig. 4D, E). Interestingly, the aberrant network formation was very similar to the phenotype observed when examining the patterning of the hindbrain capillaries (Fig. 4B) and intersomitic vessels in *adr* zebrafish mutants. The hindbrain capillary network is one of the few sites in the developing animal where active angiogenesis and vascular patterning occur between 60 and 90hpf, possibly explaining why a phenotypic effect can be observed in these capillaries, but not in vessels formed prior to 60hpf.

Discussion

Alhough tRNA-synthetases are well known for their important role in protein-synthesis, only in recent years have some of these proteins been revealed to possess additional non-canonical functions [18, 34]. Recently a number of specific diseases, including neuronal, autoimmune and metabolic conditions as well as cancer, have been linked to heritable mutations in tRNA-synthetase genes (reviewed by [35]). Some of these mutations do not affect the aminoacylation activity or enzyme stability but instead seem to interfere with non-canonical functions. In mammals, previously described non-canonical functions range from transcriptional and translational control, antiapoptosis and viral assembly to extracellular roles as inflammatory, angiogenic or angiostatic cytokines [18, 34]. In addition, fragments of Tyrosine- and Tryptophane- tRNA-Synthetases have been shown to elicit angiogenic or angiostatic responses in endothelial cells [17, 24, 36-38].

Since deletion of tRNA-synthetase genes also interferes with their essential aminoacylation activity and therefore impairs survival, the ability to uncover these non-canonical functions has been limited. So far, no specific non-canonical function of Sars has been discovered. A significant advantage of analyzing the roles of tRNA-synthetases in zebrafish is the maternal provision of mRNA[39] and/or protein, allowing for normal development during early stages. This maternal contribution is likely the reason that all described zebrafish tRNA-synthetase mutants are viable until 5dpf [30]. Therefore, maternal supply of *Sars* might also account for the relatively late onset of the vascular specific phenotype, and the confinement of the aberrant sprouting to sites of late-onset angiogenesis.

adr mutants show two different vascular specific phenotypes: a pronounced dilatation of the aortic arches (and to a lesser degree other head vessels) and the aberrant sprouting of the brain capillaries and intersomitic vessels. These different phenotypes might reflect the developmental stage of the different vessels at the time point of loss of Sars. Whereas the aortic arches are stable, previously established vessels, the brain capillaries are undergoing active angiogenesis.

Trying to distinguish between the different roles of Sars in protein synthesis and the development of the vasculature, we blocked protein synthesis for the 12 hours during which the dilatation phenotype starts to manifest itself in *adr* mutants. Although inhibition of protein synthesis did not cause *adr/sars* like phenotypes, one should consider that cycloheximide is also blocking mitochondrial protein synthesis whereas the *adr* mutation is not. [The zebrafish genome, like other vertebrate genomes, contains a complete set of mitochondrial specific tRNA-synthetases, including mitochondrial Seryl-tRNA synthetase.] On the other hand, loss of other tRNA-synthetases in zebrafish [30] or inhibition of canonical Sars function did not cause *adr/sars* like vascular phenotypes, arguing that a previously unknown direct function of Sars on endothelial cells is impaired.

However, we also analyzed the extracellular matrix as it contains serine rich proteins likely to affect the vasculature. For example, microfibrils and associated proteins have been shown to play a role in vascular development [40, 41, 42]. Therefore, we examined wild-type and *adr* mutants by immunohistochemistry, but found no obvious difference in Fibronectin or Laminin deposition. Additionally, the tube formation assay we used to analyze SARS function in HUVEC cultures is based on supplying the extra cellular matrix components in form of a basement membrane extract. If the *adr* phenotype was based on extracellular matrix deficiency, it probably could not have been phenocopied by SARS-deficient HUVEC cultures.

Taken together our observations in zebrafish and human endothelial cells indicate that Sars possesses an angiogenesis regulating capacity, with different effects representing the different developmental stages of the endothelial cells affected. Since regulation of angiogenesis is still a poorly understood subject with high medical relevance we hope that uncovering this new non-canonical function of Sars will pave the way for further insights into regulatory pathways controlling angiogenesis.

Acknowledgments

We thank Ralf Adams, Xiang-Lei Yang and Paul Schimmel for discussions, Hajime Fukui and Atsuo Kawahara for discussion and sharing unpublished data, Ralf Adams for critical comments on the manuscript and Jana Hermes for her help with the cell proliferation assays.

Sources of Funding: Support for this research came from postdoctoral fellowships from the American Heart Association (W.H.), and the Human Frontier Science Program (J.H.), and from grants from the NIH (NHLBI) and Packard Foundation (D.Y.R.S).

References

1. Jin SW, H W, Santoro MM, Mitchell TS, Frantsve J, Jungblut B, Beis D, Scott IC, D'Amico LA, Ober EA, Verkade H, Field HA, Chi NC, Wehman AM, Baier H, Stainier DY. A transgene-assisted genetic screen identifies essential regulators of vascular development in vertebrate embryos. Dev Biol 2007;307:29–42. [PubMed: 17531218]
2. Carmeliet P. Angiogenesis in health and disease. Nat Med 2003;9:653–660. [PubMed: 12778163]
3. Carmeliet P. Angiogenesis in life, disease and medicine. Nature 2005;438:932–936. [PubMed: 16355210]
4. Lawson ND, Weinstein BM. Arteries and veins: making a difference with zebrafish. Nat Rev Genet 2002;3:674–682. [PubMed: 12209142]
5. Ny A, Autiero M, Carmeliet P. Zebrafish and Xenopus tadpoles: small animal models to study angiogenesis and lymphangiogenesis. Exp Cell Res 2006;312:684–693. [PubMed: 16309670]
6. Roman BL, Weinstein BM. Building the vertebrate vasculature: research is going swimmingly. Bioessays 2000;22:882–893. [PubMed: 10984714]
7. Stainier DY, Weinstein BM, Detrich HW 3rd, Zon LI, Fishman MC. Cloche, an early acting zebrafish gene, is required by both the endothelial and hematopoietic lineages. Development 1995;121:3141–3150. [PubMed: 7588049]

8. Stainier DY. Zebrafish genetics and vertebrate heart formation. Nat Rev Genet 2001;2:39–48. [PubMed: 11253067]
9. Sehnert AJ, Huq A, Weinstein BM, Walker C, Fishman M, Stainier DY. Cardiac troponin T is essential in sarcomere assembly and cardiac contractility. Nat Genet 2002;31:106–110. [PubMed: 11967535]
10. Jin SW, B D, Mitchell T, Chen JN, Stainier DY. Cellular and molecular analyses of vascular tube and lumen formation in zebrafish. Development 2005;132:5199–5209. [PubMed: 16251212]
11. Driever W, Solnica-Krezel L, Schier AF, Neuhauss SC, Malicki J, Stemple DL, Stainier DY, Zwartkruis F, Abdelilah S, Rangini Z, Belak J, Boggs C. A genetic screen for mutations affecting embryogenesis in zebrafish. Development 1996;123:37–46. [PubMed: 9007227]
12. Haffter P, Granato M, Brand M, Mullins MC, Hammerschmidt M, Kane DA, Odenthal J, van Eeden FJ, Jiang YJ, Heisenberg CP, Kelsh RN, Furutani-Seiki M, Vogelsang E, Beuchle D, Schach U, Fabian C, Nusslein-Volhard C. The identification of genes with unique and essential functions in the development of the zebrafish, Danio rerio. Development 1996;123:1–36. [PubMed: 9007226]
13. Amsterdam A, Burgess S, Golling G, Chen W, Sun Z, Townsend K, Farrington S, Haldi M, Hopkins N. A large-scale insertional mutagenesis screen in zebrafish. Genes Dev 1999;13:2713–2724. [PubMed: 10541557]
14. Lee SW, Cho BH, Park SG, Kim S. Aminoacyl-tRNA synthetase complexes: beyond translation. J Cell Sci 2004;117:3725–3734. [PubMed: 15286174]
15. Sampath P, Mazumder B, Seshadri V, Gerber CA, Chavatte L, Kinter M, Ting SM, Dignam JD, Kim S, Driscoll DM, Fox PL. Noncanonical function of glutamyl-prolyl-tRNA synthetase: gene-specific silencing of translation. Cell 2004;119:195–208. [PubMed: 15479637]
16. Wakasugi K, Slike BM, Hood J, Otani A, Ewalt KL, Friedlander M, Cheresh DA, Schimmel P. A human aminoacyl-tRNA synthetase as a regulator of angiogenesis. Proc Natl Acad Sci U S A 2002;99:173–177. [PubMed: 11773626]
17. Kise Y, Lee SW, Park SG, Fukai S, Sengoku T, Ishii R, Yokoyama S, Kim S, Nureki O. A short peptide insertion crucial for angiostatic activity of human tryptophanyl-tRNA synthetase. Nat Struct Mol Biol 2004;11:149–156. [PubMed: 14730354]
18. Park SG, Ewalt KL, Kim S. Functional expansion of aminoacyl-tRNA synthetases and their interacting factors: new perspectives on housekeepers. Trends Biochem Sci 2005;30:569–574. [PubMed: 16125937]
19. Kisselev LL, Wolfson AD. Aminoacyl-tRNA synthetases from higher eukaryotes. Prog Nucleic Acid Res Mol Biol 1994;48:83–142. [PubMed: 7938555]
20. Mirande M. Aminoacyl-tRNA synthetase family from prokaryotes and eukaryotes: structural domains and their implications. Prog Nucleic Acid Res Mol Biol 1991;40:95–142. [PubMed: 2031086]
21. Shiba K. Intron positions delineate the evolutionary path of a pervasively appended peptide in five human aminoacyl-tRNA synthetases. J Mol Evol 2002;55:727–733. [PubMed: 12486531]
22. Kleeman TA, Wei D, Simpson KL, First EA. Human tyrosyl-tRNA synthetase shares amino acid sequence homology with a putative cytokine. J Biol Chem 1997;272:14420–14425. [PubMed: 9162081]
23. Wakasugi K, Schimmel P. Two distinct cytokines released from a human aminoacyl-tRNA synthetase. Science 1999;284:147–151. [PubMed: 10102815]
24. Otani A, Slike BM, Dorrell MI, Hood J, Kinder K, Ewalt KL, Cheresh D, Schimmel P, Friedlander M. A fragment of human TrpRS as a potent antagonist of ocular angiogenesis. Proc Natl Acad Sci U S A 2002;99:178–183. [PubMed: 11773625]
25. Westerfield, M. The Zebrafish Book. Eugene, OR: University of Oregon Press; 1993.
26. Geisler, R. Mapping and Cloning. In: Nuesslein-Vollhard, C.; Dahm, R., editors. Zebrafish. New York: Oxford University Press; 2002.
27. Huisken J, Swoger J, Del Bene F, Wittbrodt J, Stelzer EH. Optical sectioning deep inside live embryos by selective plane illumination microscopy. Science 2004;305:1007–1009. [PubMed: 15310904]
28. Traver D, Paw BH, Poss KD, Penberthy WT, Lin S, Zon LI. Transplantation and in vivo imaging of multilineage engraftment in zebrafish bloodless mutants. Nat Immunol 2003;4:1238–1246. [PubMed: 14608381]
29. Saria A, Lundberg JM. Evans blue fluorescence: quantitative and morphological evaluation of vascular permeability in animal tissues. J Neurosci Methods 1983;8:41–49. [PubMed: 6876872]

30. Amsterdam A, Nissen RM, Sun Z, Swindell EC, Farrington S, Hopkins N. Identification of 315 genes essential for early zebrafish development. Proc Natl Acad Sci U S A 2004;101:12792–12797. [PubMed: 15256591]

31. Holzschuh J, Barrallo-Gimeno A, Ettl AK, Durr K, Knapik EW, Driever W. Noradrenergic neurons in the zebrafish hindbrain are induced by retinoic acid and require tfap2a for expression of the neurotransmitter phenotype. Development 2003;130:5741–5754. [PubMed: 14534139]

32. Landeka I, Filipic-Rocak S, Zinic B, Weygand-Durasevic I. Characterization of yeast seryl-tRNA synthetase active site mutants with improved discrimination against substrate analogues. Biochim Biophys Acta 2000;1480:160–170. [PubMed: 11004561]

33. Davis GE, Camarillo CW. An alpha 2 beta 1 integrin-dependent pinocytic mechanism involving intracellular vacuole formation and coalescence regulates capillary lumen and tube formation in three-dimensional collagen matrix. Exp Cell Res 1996;224:39–51. [PubMed: 8612690]

34. Hausmann CD, Ibba M. Aminoacyl-tRNA synthetase complexes: molecular multitasking revealed. FEMS Microbiol Rev 2008;32:705–721. [PubMed: 18522650]

35. Park SG, Schimmel P, Kim S. Aminoacyl tRNA synthetases and their connections to disease. Proc Natl Acad Sci U S A 2008;105:11043–11049. [PubMed: 18682559]

36. Wakasugi K, Slike BM, Hood J, Ewalt KL, Cheresh DA, Schimmel P. Induction of angiogenesis by a fragment of human tyrosyl-tRNA synthetase. J Biol Chem 2002;277:20124–20126. [PubMed: 11956181]

37. Tzima E, Reader JS, Irani-Tehrani M, Ewalt KL, Schwartz MA, Schimmel P. VE-cadherin links tRNA synthetase cytokine to anti-angiogenic function. J Biol Chem 2005;280:2405–2408. [PubMed: 15579907]

38. Tzima E, Schimmel P. Inhibition of tumor angiogenesis by a natural fragment of a tRNA synthetase. Trends Biochem Sci 2006;31:7–10. [PubMed: 16297628]

39. Thisse B, Thisse C. Fast Release Clones: A High Throughput Expression Analysis.

40. Chen E, Larson JD, Ekker SC. Functional analysis of zebrafish microfibril-associated glycoprotein-1 (Magp1) in vivo reveals roles for microfibrils in vascular development and function. Blood 2006;107:4364–4374. [PubMed: 16469878]

41. Gansner JM, Madsen EC, Mecham RP, Gitlin JD. Essential role for fibrillin-2 in zebrafish notochord and vascular morphogenesis. Dev Dyn 2008;237:2844–2861. [PubMed: 18816837]

42. Carta L, Pereira L, Arteaga-Solis E, Lee-Arteaga SY, Lenart B, Starcher B, Merkel CA, Sukoyan M, Kerkis A, Hazeki N, Keene DR, Sakai LY, Ramirez F. Fibrillins 1 and 2 perform partially overlapping functions during aortic development. J Biol Chem 2006;281:8016–8023. [PubMed: 16407178]

43. Isogai S, Horiguchi M, Weinstein BM. The vascular anatomy of the developing zebrafish: an atlas of embryonic and early larval development. Dev Biol 2001;230:278–301. [PubMed: 11161578]

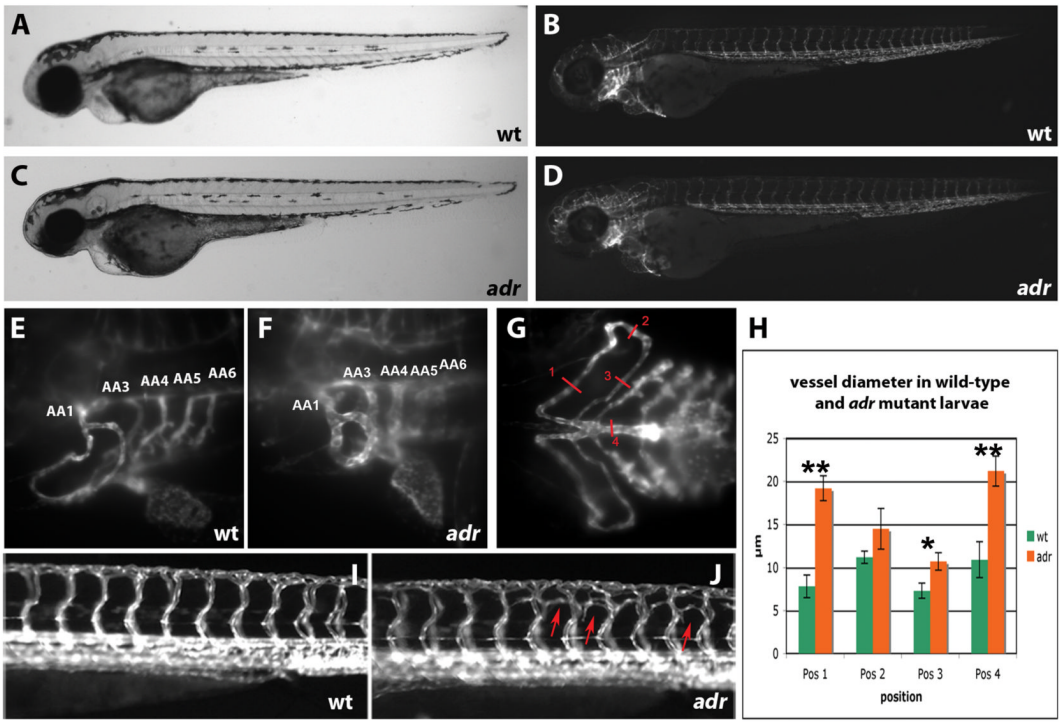

Figure 1.

(A-G) Bright-field (A and C), epifluorescence (B and D) and SPIM (E - G) micrographs of 80hpf wild-type (A, B, E, and G) and *adr*^{s277} mutant (C, D, and F) *Tg(flk1:EGFP)*^{s843} larvae, shown in lateral (A to F) and ventral (G) views. At this stage, the mutants resemble their wild-type siblings except for the dilatation of the aortic arch vessels (numbered AA1-6, the vestigial AA2[43] is not visible).

(H) Diagram showing the diameter of the aortic arch vessels in wild-type (n = 4) and *adr*^{s277} mutant (n = 4) larvae measured at the positions indicated in G. Error bars show the standard deviation. The P value was considered statistically significant and marked by ** when (P< 0.01) and by * when (P< 0.05).

(I, J) Epifluorescence micrographs of 82hpf wild-type (I) and *adr*^{s277} mutant (J) *Tg (flk1:EGFP)*^{s843} larvae shown in lateral views. The intersomitic vessels in *adr* mutants exhibit ectopic branching (indicated by red arrows), especially in the dorsal half of the myotome.

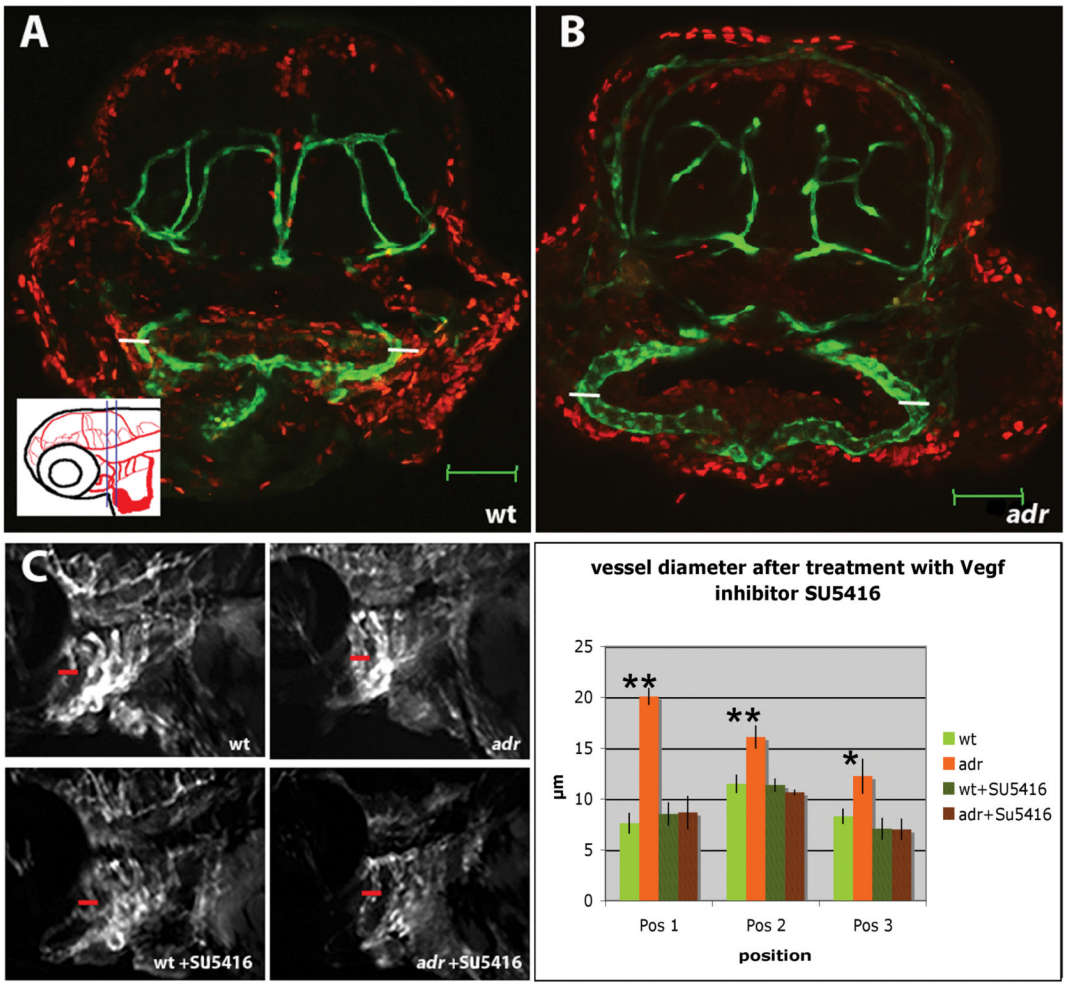

Figure 2.

(A, B) Confocal crossections of 74hpf wild-type (A) and *adr*^{s277} mutant (B) larvae visualized for *Tg(flk1:*EGFP)^{s843} expression (green) and BrdU (red).

BrdU labeling indicates that no cell proliferation takes place between 59 and 74hpf within the endothelial cells (GFP-positive) of the 2nd visible aortic arch vessel (AA3) of wild-type (A) or *adr*^{s277} mutant (B) animals. Also note the clear dilatation of the aortic arch vessel (small white bars corresponding to 25µm in A and B). Scale bars, 50µm.

(C, D) Treatment of wild-type and *adr* mutant animals with the VegfR inhibitor SU5416 from 60hpf to 76hpf. (C) Epifluorescence micrographs of 76hpf untreated and SU5416 treated wild-type and *adr*^{s277} mutant larvae (red bars indicate the aortic arch diameter of untreated *adr* mutant larvae). (D) Diagram showing the diameter of the aortic arch vessel (AA1) in untreated and SU5416 treated wild-type and *adr*^{s277} mutant larvae. The aortic arch vessel diameter was measured at the positions indicated in Fig. 1G (4 wild-types, 3 mutants, 4-5 SU5416 treated wild-types and 3-6 SU5416 treated mutants were examined; for these latter two groups not all positions were easily visible in all embryos).

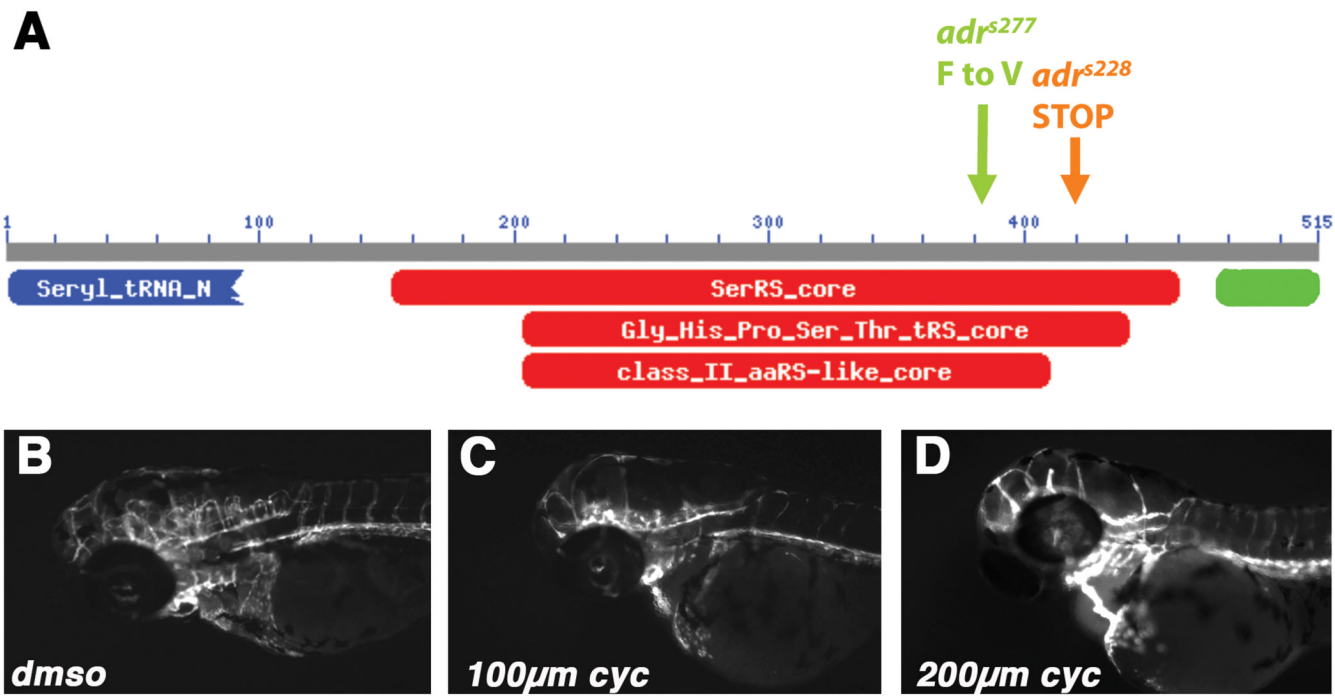

Figure 3.

(A) Schematic representation of the Seryl-tRNA synthetase protein and the location of the lesions in the two mutant alleles Sars^{s277} and Sars^{s228}. The blue bar outlines a highly homologous area containing the serine-recognition site, the red bar the conserved enzymatic core, and the green bar the vertebrate-specific C-terminal appendage.

(B-D) Cycloheximide (cyc) treatment of zebrafish embryos between 60 and 72hpf; epifluorescence micrographs of DMSO-control (B), 100μM cyc (C) and 200μM cyc (D) treated larvae visualized for *Tg(flk1:*EGFP)^{s843} expression.

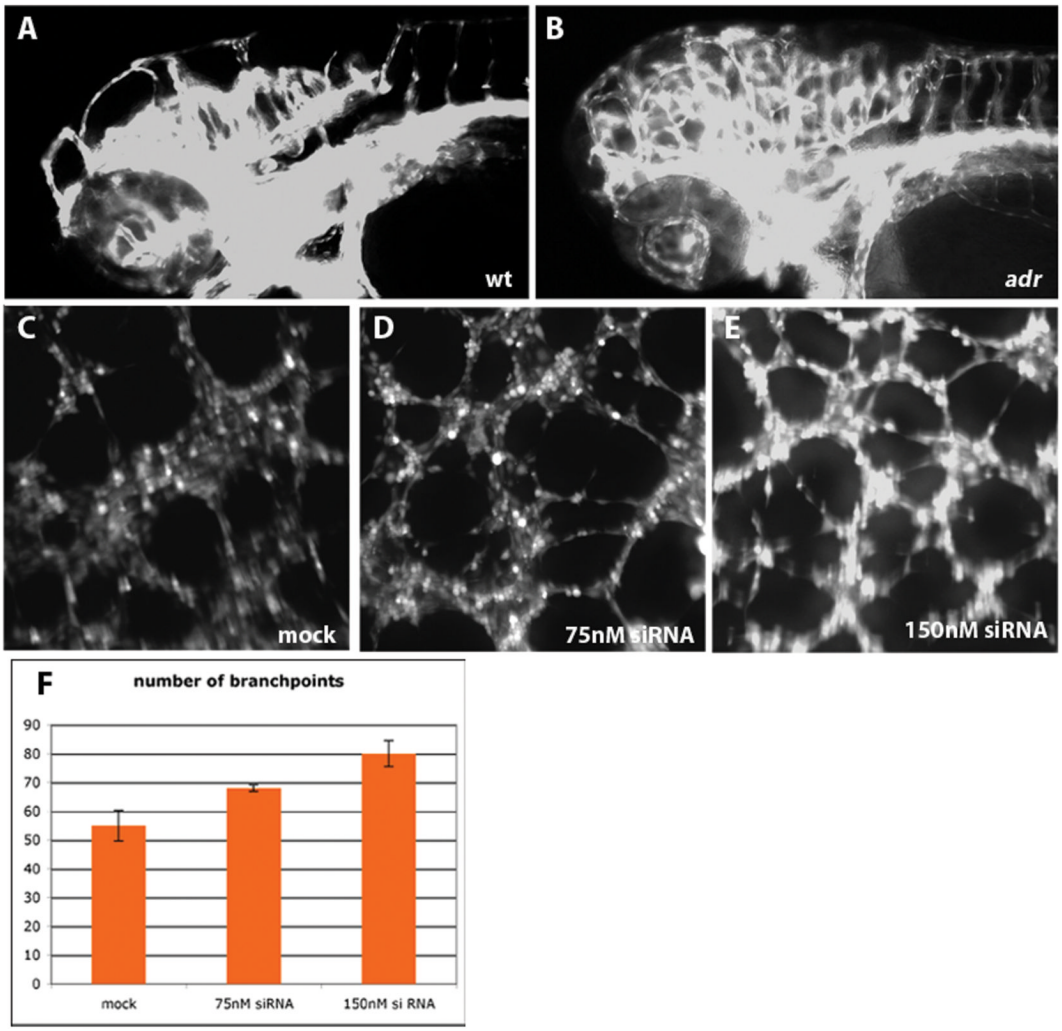

Figure 4.

Loss of Sars leads to increased sprouting in actively forming vessels.

(A, B) Aberrant vessel formation in hindbrain capillaries of *adr*^{s277} mutants (B, compare to wild-type in A). Epifluorescence micrographs of 80hpf wild-type (A) and *adr*^{s277} mutant (B) *Tg(flk1:EGFP)*^{s843} larvae, shown in lateral views. These micrographs were overexposed to reveal all the vascular branches.

(C-E) Knockdown of *SARS* in human endothelial cells.

Mock (C) and *SARS*-siRNA (D, E) transfected HUVEC's visualized by Calcein staining after a tube formation assay.

(H) Number of branchpoints in the vascular network formed by HUVECs after either mock or siRNA transfection. Shown are the mean values, error bars denote standard deviation. P<0.05 mock vs 75nM, P<0.01 mock vs 150nM, P<0.05 75nM vs 150nM.